makes the effective room-temperature pressure 3-4 atm.

Para-enriched H_2 was generated either by storing the tubes for longer than 8 h at -196 °C or by adding para-enriched H_2 immediately before carrying out the NMR experiments. Para-enriched hydrogen can be readily prepared by storage of H_2 at -196 °C in a bulb containing Fe_2O_3/C/silica catalyst for more than 2 h.

Gas Evolution Studies. The amount of H_2 produced in the reaction of I with acids was measured as follows. Complex I was suspended in a minimum of acetone under N_2. Aqueous HCl was quickly added through a septum. Gas chromatographic measurements were made until a constant value was obtained for the H_2 pressure. Since the volume of the gas above the reaction mixture was greater than 100 mL, the withdrawl of 0.5-mL aliquots for sampling affected the total sample pressure by only 0.5%. Methane evolution was monitored in a similar fashion for the reaction of I in neat methyl iodide.

Acknowledgment. We thank the donors of the Petroleum Research Fund, administered by the American Chemical Society, and the National Science Foundation (Grant CHE 86-03055) for support of this work and the Johnson Matthey Co., Inc., for a generous load of palladium salts. We also acknowledge helpful assistance from Jeffrey Meier.

Registry No. $Pd_2Cl_2(dppm)_2$, 64345-29-5; $Pd_2(dppm)_3$, 37266-95-8; $PdI_2(dppm)$, 77462-40-9; $[Pd_2I(dppm)_2(CH_3)_2]I$, 81457-54-7; $Pd_2(\mu_2\text{-}CH_2)I_2(dppm)_2$, 78274-36-9; $Pd_2(\mu_2\text{-}CH_2)Cl_2(dppm)_2$, 78274-94-9; $[Pd_3(dppm)_3(\mu_3\text{-}CO)](CF_3CO_2)_2$, 89189-81-1; $PdCl_2(dppm)$, 38425-01-3; CH_3I, 74-88-4; CH_2I_2, 75-11-6; HCl, 7647-01-0; I_2, 7553-56-2; $(CH_3)_3SiCl$, 75-77-4; $(CH_3)_2SiCl_2$, 75-78-5; CH_4, 74-82-8; $(Me_3Si)_2O$, 107-46-0; H_2, 1333-74-0; PhC≡CH, 536-74-3; *tert*-butylacetylene, 917-92-0; 1-phenyl-1-propyne, 673-32-5; styrene-d_8, 19361-62-7; ethylene-d_4, 683-73-8.

Supplementary Material Available: Tables of data collection and refinement parameters, anisotropic thermal parameters, calculated hydrogen positional parameters, and complete bond distances and angles for non-hydrogen atoms (12 pages); a listing of observed and calculated structure factors for $Pd_2(dppm)_3$ (31 pages). Ordering information is given on any current masthead page.

Contribution from the Departamento de Quimica Inorganica, Universitat de Valencia, Blasco Ibanez No. 13, 46010 Valencia, Spain, Laboratoire de Chimie de Coordination du CNRS, 205 route de Narbonne, 31077 Toulouse Cedex, France, and Institut de Ciencia de Materials, CSIC, Marti y Franquês s/n, 08028 Barcelona, Spain

Synthesis, Characterization, and Magnetic Properties of μ-Oxalato- and μ-Oxamido-Bridged Copper(II) Dimers. Crystal and Molecular Structures of $[Cu_2(mepirizole)_2(C_2O_4)(H_2O)_2](PF_6)_2\cdot mepirizole\cdot 3H_2O$ and $[Cu_2(mepirizole)_2(C_2O_4)(NO_3)_2(H_2O)]_2[Cu_2(mepirizole)_2(C_2O_4)(NO_3)_2]$

L. Soto,[1a] J. Garcia,[1a] E. Escriva,[1a] J.-P. Legros,[1b] J.-P. Tuchagues,*[,1b] F. Dahan,[1b] and A. Fuertes[1c]

Received December 12, 1988

Four complexes, $[Cu_2L_2(ox)(H_2O)_2](PF_6)_2\cdot L\cdot 3H_2O$ (**1**), $[Cu_2L_2(ox)(NO_3)_2(H_2O)]_2[Cu_2L_2(ox)(NO_3)_2]$ (**2**), $Cu_2L_2(ox)(ClO_4)_2$ (**3**), and $Cu_2L_2(oxamd)(NO_3)_2\cdot H_2O$ (**4**), with ox = oxalato, oxamd = oxamido, and L = mepirizole (4-methoxy-2-(5-methoxy-3-methyl-pyrazol-1-yl)-6-methylpyrimidine), have been synthesized. The structures of **1** and **2** have been determined. **1** crystallizes in the orthorhombic system, space group *Pnma*, with $Z = 8$ and $a = 21.864$ (3) Å, $b = 20.881$ (5) Å, and $c = 11.451$ (3) Å. **2** crystallizes in the monoclinic system, space group $P2_1/n$, with $Z = 4$ and $a = 20.073$ (4) Å, $b = 13.842$ (4) Å, $c = 20.070$ (4) Å, and $\beta = 119.09$ (2)°. The structure of **1** consists of centrosymmetric binuclear cations $[L(H_2O)Cu(ox)Cu(H_2O)L]^{2+}$ separated by PF_6^- anions and molecules of free mepirizole and water of crystallization. The structure of **2** is composed of two crystallographically independent dimers $[L(NO_3)Cu(ox)Cu(NO_3)(H_2O)L]$ and $[L(NO_3)Cu(ox)Cu(NO_3)L]$. The four complexes have been studied with IR, UV-visible, and EPR spectroscopies and magnetic susceptibility measurements in the 360-5 K range. The four complexes exhibit strong antiferromagnetic exchange interactions ranging from -156 to -201 cm^{-1}. Magnetic and EPR results are discussed with respect to the crystal structures of **1** and **2**.

Introduction

It is now well-known that multiatom bridges can propagate magnetic exchange interactions between paramagnetic metal ions.[2] The dependence of the magnetic exchange upon the nature of the bridging species and/or stereochemical factors has been the subject of several recent studies.[3-5]

The oxalato anion and related groups as oxamido, oxamato, etc., have been incorporated as bis-bidentate bridges into complexes containing a variety of metal ions. However the factors controlling the magnitude of superexchange interactions have been best illustrated with copper(II) complexes.[2,3] Only net antiferromagnetic interactions have been observed in these complexes, the magnitude of which basically depends upon two factors: (i) the nature and magnitude of the overlap between the metal d orbitals containing the unpaired electrons and the bridging ligand orbitals; (ii) the energy difference between the two magnetic orbitals.

In this paper, we report the synthesis, characterization, and structural and magnetic study of three copper-oxalato (ox) complexes and one copper-oxamido (oxamd) complex containing the binuclear $[LCu(ox)CuL]^{2+}$ and $[LCu(oxamd)CuL]^{2+}$ entities, respectively. Mepirizole (4-methoxy-2-(5-methoxy-3-methyl-pyrazol-1-yl)-6-methylpyrimidine, herein abbreviated L), a biologically active compound,[6] has been used as terminal ligand in these new materials. This ligand, including both the pyrimidyl

* Author to whom correspondence should be addressed.

(1) (a) Universitat de Valencia. (b) Laboratoire de Chimie de Coordination du CNRS. (c) Institut de Ciencia de Materials.

(2) Willett, R. D., Gatteschi, D., Kahn, O. Eds. *Magneto-structural Correlations in Exchange-Coupled Systems*; NATO ASI Series; Reidel: Dordrecht, Holland, 1985.
(3) Kahn, O. *Angew. Chem., Int. Ed. Engl.* **1985**, *24*, 834-850.
(4) Murray, K. S. In *Biological and Inorganic Copper Chemistry*; Carlin, K. D., Zubieta, J., Eds.; Academic Press, New York, 1986; Vol. 2.
(5) Charlot, M. F.; Kahn, O.; Chaillet, M.; Larrieu, C. *J. Am. Chem. Soc.* **1986**, *108*, 2574-2581.
(6) Takabataka, E.; Kodama, R.; Tanaka, Y.; Dohmori, R.; Tachizanawa, H.; Naito, P. *Chem. Pharm. Bull.* **1970**, *18*, 1900.
(7) (a) Molla, M. C.; Garcia, J.; Borras, J.; Foces, C.; Cano, F. H.; Martinez, M. *Transition Met. Chem. (Weinheim, Ger.)* **1985**, *10*, 460-463. (b) Soto, L.; Legros, J. P.; Molla, M. C.; Garcia, J. *Acta Crystallogr.* **1987**, *C43*, 834-836. (c) Suarez-Varela, J.; Soto, L.; Legros, J. P.; Esteve, C.; Garcia, J. *Polyhedron* **1988**, *7*, 229-234.

0020-1669/89/1328-3378$01.50/0

Table I. Crystallographic Data for **1** and **2**

	1	2
formula of the asymmetric unit	$C_{17.5}H_{26}CuF_6N_6O_{7.5}P$	$C_{36}H_{44}Cu_3N_{15}O_{22}$
fw	648.9	1229.5
a, Å	21.864 (3)	20.073 (4)
b, Å	20.881 (5)	13.842 (4)
c, Å	11.451 (3)	20.070 (4)
β, deg		119.09 (2)
V, Å^3	5528 (3)	4873 (4)
space group	*Pnma* (No. 62)	$P2_1/n$ (No. 11)
Z	8	4
d_{obsd}, g cm^{-3} (flotation)	1.64 (2)	1.66 (2)
d_{calcd}, g cm^{-3}	1.65	1.68
temp, K	295	295
radiation	Mo Kα, λ = 0.71069 Å, graphite monochromator	
μ(Mo Kα), cm^{-1}	9.9	14.0
$R = \sum\|k\|F_o\| - \|F_c\|\|/\sum k\|F_o\|$	0.081	0.047
$R_w = [\sum w(k\|F_o\| - \|F_c\|)^2/\sum wk^2F_o^2]^{1/2}$	0.090	0.050

Table II. Non-Hydrogen Atom Positional Parameters and Isotropic or Equivalent Thermal Parameters (Å^2 × 100) for Complex **1**

atom	x/a	y/b	z/c	U_{eq}/U_{iso}
Cu	0.57126 (7)	0.43491 (8)	0.13588 (14)	5.0 (3)
N(1)	0.6619 (5)	0.4221 (5)	0.1588 (9)	5 (2)
C(2)	0.6775 (6)	0.4169 (6)	0.2711 (11)	4 (2)
N(3)	0.7339 (6)	0.4112 (6)	0.3187 (12)	7 (3)
C(4)	0.7742 (8)	0.4122 (7)	0.2422 (20)	8 (4)
C(5)	0.7676 (7)	0.4163 (7)	0.1269 (14)	6 (3)
C(6)	0.7100 (7)	0.4213 (7)	0.0853 (12)	6 (3)
N(7)	0.6295 (5)	0.4165 (6)	0.3512 (9)	5 (2)
N(8)	0.5701 (5)	0.4189 (5)	0.3061 (9)	5 (2)
C(9)	0.5319 (6)	0.4175 (7)	0.3939 (13)	5 (3)
C(10)	0.5638 (8)	0.4151 (7)	0.5007 (13)	7 (3)
C(11)	0.6267 (8)	0.4155 (8)	0.4713 (14)	8 (4)
O(12)	0.6739 (6)	0.4131 (7)	0.5312 (10)	10 (3)
C(13)	0.6673 (9)	0.4139 (9)	0.6562 (9)	12 (4)
C(14)	0.4643 (6)	0.4195 (7)	0.3777 (14)	7 (3)
O(15)	0.8345 (5)	0.4049 (6)	0.2831 (11)	10 (3)
C(16)	0.8427 (7)	0.3924 (10)	0.3996 (15)	9 (4)
C(17)	0.6997 (7)	0.4232 (8)	−0.0448 (11)	8 (3)
O(18)	0.5760 (4)	0.4788 (5)	−0.0171 (8)	6 (2)
C(19)	0.5264 (6)	0.5050 (7)	−0.0425 (11)	5 (3)
O(20)	0.4851 (4)	0.4614 (5)	0.1291 (8)	7 (2)
O(1)W	0.5539 (5)	0.3369 (5)	0.0632 (10)	8 (2)
N(21)	0.3918 (7)	3/4	0.7325 (14)	5.2 (4)
C(22)	0.3307 (8)	3/4	0.7263 (15)	3.9 (4)
N(23)	0.2960 (6)	3/4	0.6314 (14)	5.0 (4)
C(24)	0.3273 (10)	3/4	0.5363 (19)	6.2 (6)
C(25)	0.3867 (9)	3/4	0.5278 (18)	6.1 (6)
C(26)	0.4194 (9)	3/4	0.6278 (19)	6.0 (5)
N(27)	0.3005 (7)	3/4	0.8333 (13)	5.0 (4)
N(28)	0.3334 (7)	3/4	0.9355 (14)	6.0 (5)
C(29)	0.2895 (10)	3/4	1.0173 (18)	5.8 (6)
C(30)	0.2348 (10)	3/4	0.9794 (19)	7.1 (6)
C(31)	0.2383 (9)	3/4	0.8623 (20)	6.3 (6)
O(32)	0.1995 (7)	3/4	0.7759 (13)	7.6 (4)
C(33)	0.1364 (10)	3/4	0.8197 (22)	10.3 (9)
C(34)	0.3123 (11)	3/4	1.1448 (20)	10.1 (8)
O(35)	0.2958 (8)	3/4	0.4322 (14)	8.5 (5)
C(36)	0.2342 (11)	3/4	0.4365 (23)	10.6 (9)
C(37)	0.4864 (9)	3/4	0.6315 (21)	8.1 (7)
O(2)W	0.5500 (12)	3/4	0.9718 (23)	18 (1)
O(3)W	0.5448 (9)	0.1688 (10)	0.8169 (18)	21.6 (9)
P	0.88057 (21)	0.38773 (22)	0.7738 (4)	7.0 (8)
F(1)	0.8646 (6)	0.4355 (6)	0.8764 (9)	16.1 (5)
F(2)	0.8948 (6)	0.3381 (5)	0.6733 (9)	15.5 (5)
F(3)	0.9351 (9)	0.4308 (10)	0.7290 (24)	18.5 (9)
F(4)	0.8241 (7)	0.3450 (8)	0.8103 (18)	13.9 (7)
F(5)	0.9288 (7)	0.3460 (8)	0.8428 (14)	12.9 (6)
F(6)	0.8365 (8)	0.4307 (8)	0.6975 (13)	13.6 (6)
F(3)X	0.8917 (22)	0.4383 (15)	0.6733 (26)	13 (1)
F(4)X	0.9471 (7)	0.4081 (19)	0.813 (3)	10 (1)
F(5)X	0.8856 (23)	0.3385 (17)	0.8782 (26)	13 (2)
F(6)X	0.8125 (9)	0.369 (3)	0.742 (5)	18 (2)

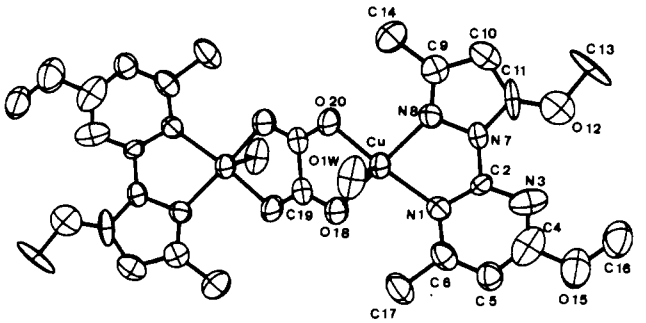

Figure 1. Projection of the $[Cu_2L_2(ox)(H_2O)_2]^{2+}$ cation of **1** onto the (010) plane. The numbering scheme for the free mepirizole molecule is obtained by adding 20. H atoms are omitted; ellipsoids are scaled to enclose 50% probability.

and pyrazole rings, has been shown to act as a bidentate ligand through two nitrogen atoms, one from each ring, with significant steric hindrance in the formation of metal complexes.[7]

Experimental Section

Materials. The mepirizole ligand (Daiichi Seiyaku Co. Japan) was purified by crystallization from methanol. All other reagents were used as received.

Syntheses. $[Cu_2L_2(ox)(H_2O)_2](PF_6)_2\cdot L\cdot 3H_2O$ (1) (L = Mepirizole). An aqueous solution of KPF_6 (30 mmol; 50 mL) was added to an aqueous mixture of $Cu(NO_3)_2\cdot 3H_2O$ (20 mmol; 50 mL), mepirizole (30 mmol; 50 mL), and $Na_2C_2O_4$ (10 mmol; 50 mL). The resulting green-blue crystals were separated by filtration and washed with water and ethanol. Anal. Calcd for $C_{35}H_{52}N_{12}O_{15}F_{12}P_2Cu_2$: C, 32.39; H, 4.04; N, 12.95; Cu, 9.79. Found: C, 32.10; H, 3.90; N, 13.10; Cu, 9.89.

$[Cu_2L_2(ox)(NO_3)_2(H_2O)]_2[Cu_2L_2(ox)(NO_3)_2]$ (2). An ethanolic solution (50 mL) of mepirizole (80 mmol) and an aqueous solution (50 mL) of $Na_2C_2O_4$ (40 mmol) were added to aqueous copper(II) nitrate (100 mL; 40 mmol). The resulting green-blue crystals were separated by filtration and washed with water and ethanol. Anal. Calcd for $C_{72}H_{88}N_{30}O_{44}Cu_6$: C, 35.18; H, 3.60; N, 17.10; Cu, 15.51. Found: C, 35.00; H, 3.80; N, 17.20; Cu, 15.40.

$Cu_2L_2(ox)(ClO_4)_2$ (3). This complex was synthesized according to the procedure described by Garcia et al.[8]

$Cu_2L_2(oxamd)(NO_3)_2\cdot H_2O$ (4). $LiOH\cdot H_2O$ (0.42 g) was dissolved in a small volume of water and added to a warm (60 °C) mixture of $Cu(NO_3)_2\cdot 3H_2O$ (2.42 g), H_2oxamd (0.44 g), and mepirizole (2.34 g) in 200 mL of water, yielding a green solution. The resulting precipitate was washed with water and dried to constant weight. Anal. Calcd for $C_{24}H_{32}N_{12}O_{13}Cu_2$: C, 35.00; H, 3.92; N, 20.41; Cu, 15.43. Found: C, 35.00; H, 3.80; N, 20.00; Cu, 15.30.

X-ray Crystallographic Studies of 1 and 2. Crystal data and relevant informations about data collection and refinement for **1** and **2** are given in Tables I and VII.[9] In both cases, the intensities of three standard reflections were monitored throughout the data collection. No significant fluctuation was noticed. The usual Lorentz–polarization factors were applied to the net intensities. Absorption corrections were estimated to be unnecessary on the basis of small μ's and blocklike shapes of the crystals. All calculations were performed by using standard program packages.[10-14] Patterson and direct methods were used in parallel to set up a trial model. In subsequent least-squares refinements, scattering factors were taken from ref 15 and anomalous dispersion corrections were applied to non-hydrogen atoms. Further details are given below for each individual complex.

(8) Tormos, J. G.; Molla, M. C.; Garcia, J. *Synth. React. Inorg. Met.-Org. Chem.* **1986**, *16*, 821–829.
(9) Supplementary material.
(10) Main, P.; Hull, S. E.; Lessinger, L.; Germain, G.; Declercq, J.-P.; Woolfson, M. H. "MULTAN 78, a System of Computer Programs for the Automatic Solution of Crystal Structures from X-ray Diffraction Data"; Universities of York, England, and Louvain, Belgium, 1978.
(11) *Structure Determination Package*; Enraf-Nonius: Delft, The Netherlands, 1979.
(12) Sheldrick, G. M. "SHELXS-86, Program for Crystal Structure Solution"; University of Göttingen, 1986.
(13) Sheldrick, G. M. "SHELX, a Program for Crystal Structure Solution"; University Chemical Laboratory: Cambridge, England, 1976.
(14) Johnson, C. K. "ORTEP"; Report ORNL-3794; Oak Ridge National Laboratory: Oak Ridge, TN, 1965.
(15) *International Tables for X-ray Crystallography*; Kynoch: Birmingham, England, 1974.

Table III. Selected Interatomic Distances (Å) and Bond Angles (deg) for Complex **1**[a]

Coordination Sphere			
Cu–N(1)	2.02 (1)	Cu–O(20)	1.964 (9)
Cu–N(8)	1.98 (1)	Cu–O(1)W	2.24 (1)
Cu–O(18)	1.979 (9)		
N(1)–Cu–O(20)	169.9 (4)	N(1)–Cu–N(8)	82.1 (4)
N(1)–Cu–O(1)W	95.4 (4)	N(1)–Cu–O(18)	97.2 (4)
N(8)–Cu–O(18)	162.0 (4)	N(8)–Cu–O(20)	94.3 (4)
N(8)–Cu–O(1)W	102.1 (4)	O(18)–Cu–O(20)	83.4 (4)
O(18)–Cu–O(1)W	95.9 (4)	O(20)–Cu–O(1)W	94.6 (4)
Oxalato Bridge			
O(18)–C(19)	1.25 (2)	O(18)–C(19)–C(19)^{i}	117 (1)
C(19)–C(19)^{i}	1.52 (2)	O(18)–C(19)–O(20)	128 (1)
C(19)–O(20)	1.24 (2)	C(19)^{i}–C(19)–O(20)	116 (1)
Coordinated Mepirizole			
N(1)–C(2)	1.33 (2)	N(7)–N(8)	1.40 (2)
N(1)–C(6)	1.35 (2)	N(7)–C(11)	1.38 (2)
C(2)–N(3)	1.35 (2)	N(8)–C(9)	1.31 (2)
C(2)–N(7)	1.39 (2)	C(9)–C(10)	1.41 (2)
N(3)–C(4)	1.24 (2)	C(9)–C(14)	1.49 (2)
C(4)–C(5)	1.33 (3)	C(10)–C(11)	1.42 (2)
C(4)–O(15)	1.41 (2)	C(11)–O(12)	1.24 (2)
C(5)–C(6)	1.35 (2)	O(12)–C(13)	1.44 (2)
C(6)–C(17)	1.51 (2)	O(15)–C(16)	1.37 (2)
C(2)–N(1)–C(6)	114 (1)	C(2)–N(7)–C(11)	134 (1)
N(1)–C(2)–N(3)	129 (1)	N(8)–N(7)–C(11)	109 (1)
N(1)–C(2)–N(7)	116 (1)	N(7)–N(8)–C(9)	108 (1)
N(3)–C(2)–N(7)	115 (1)	C(10)–C(9)–C(14)	127 (1)
C(2)–N(3)–C(4)	111 (1)	N(8)–C(9)–C(10)	111 (1)
N(3)–C(4)–O(15)	115 (2)	N(8)–C(9)–C(14)	122 (1)
N(3)–C(4)–C(5)	129 (2)	C(9)–C(10)–C(11)	106 (1)
C(5)–C(4)–O(15)	116 (2)	N(7)–C(11)–C(10)	106 (1)
C(4)–C(5)–C(6)	117 (1)	N(7)–C(11)–O(12)	121 (2)
N(1)–C(6)–C(5)	121 (1)	C(10)–C(11)–O(12)	133 (2)
N(1)–C(6)–C(17)	120 (1)	C(11)–O(12)–C(13)	118 (1)
C(5)–C(6)–C(17)	119 (1)	C(4)–O(15)–C(16)	118 (1)
C(2)–N(7)–N(8)	117 (1)		
Noncoordinated Mepirizole			
N(21)–C(22)	1.34 (2)	N(27)–N(28)	1.37 (2)
N(21)–C(26)	1.34 (3)	N(27)–C(31)	1.40 (3)
C(22)–N(23)	1.33 (2)	N(28)–C(29)	1.34 (3)
C(22)–N(27)	1.39 (2)	C(29)–C(30)	1.27 (3)
N(23)–C(24)	1.29 (3)	C(29)–C(34)	1.54 (3)
C(24)–C(25)	1.30 (3)	C(30)–C(31)	1.34 (3)
C(24)–O(35)	1.38 (2)	C(31)–O(32)	1.30 (3)
C(25)–C(26)	1.35 (3)	O(32)–C(33)	1.47 (3)
C(26)–C(37)	1.47 (3)	O(35)–C(36)	1.35 (3)
C(22)–N(21)–C(26)	114 (2)	C(22)–N(27)–C(31)	132 (2)
N(21)–C(22)–N(23)	128 (2)	N(28)–N(27)–C(31)	108 (2)
N(21)–C(22)–N(27)	115 (2)	N(27)–N(28)–C(29)	103 (2)
N(23)–C(22)–N(27)	117 (2)	N(28)–C(29)–C(30)	116 (2)
C(22)–N(23)–C(24)	113 (2)	N(28)–C(29)–C(34)	115 (2)
N(23)–C(24)–C(25)	126 (2)	C(30)–C(29)–C(34)	129 (2)
N(23)–C(24)–O(35)	118 (2)	C(29)–C(30)–C(31)	107 (2)
C(25)–C(24)–O(35)	116 (2)	N(27)–C(31)–C(30)	107 (2)
C(24)–C(25)–C(26)	118 (2)	N(27)–C(31)–O(32)	117 (2)
N(21)–C(26)–C(37)	115 (2)	C(30)–C(31)–O(32)	136 (2)
N(21)–C(26)–C(25)	121 (2)	C(31)–O(32)–C(33)	111 (2)
C(25)–C(26)–C(37)	124 (2)	C(24)–O(35)–C(36)	118 (2)
C(22)–N(27)–N(28)	120 (1)		

[a] Superscript i indicates an inversion through a center of symmetry.

Complex 1. Space group in *Pnma* or $Pna2_1$. Least-squares refinements were conducted in the centrosymmetric space group *Pnma* on the basis of convincing intensity statistics.[16] All non-hydrogen atoms of the complex ion were assigned anisotropic thermal parameters. A molecule of uncoordinated ligand (L) lying as a whole in a crystallographic mirror was given isotropic thermal parameters for all atoms. Hydrogen atoms (except those of the water molecules which could not be located) were included in the calculations by using idealized positions (C–H = 0.97 Å) and arbitrary isotropic temperature factors (U = 0.07 Å^2). The PF_6^-

(16) Howells, E. R.; Phillips, D. C.; Rogers, D. *Acta Crystallogr.* **1950**, *3*, 210–213.

Table IV. Non-Hydrogen Atom Positional Parameters and Isotropic or Equivalent Thermal Parameters (Å^2 × 100) for Complex **2**

atom	x/a	y/b	z/c	U_{eq}/U_{iso}
Cu(1)	0.91869 (4)	0.35611 (7)	0.31628 (5)	4.4 (2)
Cu(2)	0.62731 (4)	0.37388 (7)	0.20325 (5)	4.2 (2)
O(91)	0.8284 (3)	0.3430 (4)	0.2174 (3)	6 (1)
O(92)	0.8452 (3)	0.3466 (5)	0.3553 (3)	6 (1)
O(93)	0.7023 (3)	0.3564 (5)	0.1677 (3)	6 (1)
O(94)	0.7188 (3)	0.3568 (4)	0.3069 (3)	5 (1)
C(91)	0.7681 (4)	0.3513 (6)	0.2219 (4)	5 (1)
C(92)	0.7782 (4)	0.3517 (6)	0.3017 (4)	4 (1)
N(1)	0.9989 (3)	0.3819 (4)	0.2839 (3)	4 (1)
C(2)	1.0682 (4)	0.3862 (5)	0.3419 (4)	4 (1)
N(3)	1.1337 (3)	0.3965 (4)	0.3422 (3)	4 (1)
C(4)	1.1283 (4)	0.3981 (6)	0.2746 (4)	5 (1)
C(5)	1.0594 (4)	0.3931 (6)	0.2082 (4)	5 (1)
C(6)	0.9943 (4)	0.3844 (6)	0.2136 (4)	5 (1)
N(7)	1.0735 (3)	0.3814 (5)	0.4143 (3)	4 (1)
N(8)	1.0060 (3)	0.3779 (4)	0.4174 (3)	4 (1)
C(9)	1.0279 (4)	0.3742 (5)	0.4914 (4)	4 (1)
C(10)	1.1062 (4)	0.3743 (6)	0.5359 (4)	4 (1)
C(11)	1.1342 (4)	0.3777 (5)	0.4861 (4)	4 (1)
O(12)	1.2048 (3)	0.3762 (4)	0.4968 (3)	5.2 (9)
C(13)	1.2627 (4)	0.3602 (8)	0.5745 (4)	7 (2)
C(14)	0.9712 (4)	0.3729 (6)	0.5200 (4)	5 (1)
O(15)	1.1913 (3)	0.4080 (4)	0.2689 (3)	6 (1)
C(16)	1.2629 (4)	0.4126 (7)	0.3384 (5)	6 (2)
C(17)	0.9189 (4)	0.3770 (8)	0.1449 (4)	7 (2)
N(21)	0.5386 (3)	0.3844 (4)	0.2260 (3)	4 (1)
C(22)	0.4706 (3)	0.3778 (5)	0.1638 (4)	4 (1)
N(23)	0.4019 (3)	0.3778 (5)	0.1581 (3)	5 (1)
C(24)	0.4031 (4)	0.3856 (6)	0.2239 (4)	5 (1)
C(25)	0.4675 (4)	0.3932 (6)	0.2919 (4)	5 (1)
C(26)	0.5364 (4)	0.3941 (6)	0.2924 (4)	5 (1)
N(27)	0.4716 (3)	0.3723 (5)	0.0946 (3)	4 (1)
N(28)	0.5424 (3)	0.3752 (4)	0.0982 (3)	4 (1)
C(29)	0.5268 (4)	0.3767 (6)	0.0253 (4)	4 (1)
C(30)	0.4489 (4)	0.3744 (6)	−0.0249 (4)	5 (1)
C(31)	0.4147 (4)	0.3727 (6)	0.0202 (4)	4 (1)
O(32)	0.3430 (3)	0.3712 (5)	0.0042 (3)	6 (1)
C(33)	0.2885 (4)	0.3729 (8)	−0.0754 (4)	7 (2)
C(34)	0.5885 (4)	0.3795 (6)	0.0039 (4)	6 (2)
O(35)	0.3356 (3)	0.3848 (4)	0.2233 (3)	6 (1)
C(36)	0.2671 (4)	0.3823 (7)	0.1525 (5)	7 (2)
C(37)	0.6086 (4)	0.4080 (8)	0.3636 (4)	7 (2)
Cu(3)	1.08639 (5)	0.64599 (7)	0.07924 (5)	4.3 (2)
O(95)	1.0966 (3)	0.5013 (4)	0.0626 (3)	5 (1)
O(96)	0.9807 (3)	0.6212 (5)	0.0010 (3)	6 (1)
C(93)	1.0335 (4)	0.4668 (6)	0.0178 (4)	4 (1)
N(41)	0.9136 (3)	0.3556 (5)	−0.1889 (3)	4 (1)
C(42)	0.8443 (4)	0.3557 (5)	−0.2480 (4)	4 (1)
N(43)	0.8214 (3)	0.3592 (5)	−0.3224 (4)	5 (1)
C(44)	0.8776 (4)	0.3638 (6)	−0.3376 (4)	5 (1)
C(45)	0.9534 (4)	0.3633 (6)	−0.2820 (4)	5 (1)
C(46)	0.9706 (4)	0.3579 (6)	−0.2080 (4)	5 (1)
N(47)	0.7847 (3)	0.3499 (4)	−0.2296 (3)	4 (1)
N(48)	0.8043 (3)	0.3491 (4)	−0.1536 (3)	4 (1)
C(49)	0.7392 (4)	0.3522 (6)	−0.1515 (4)	5 (1)
C(50)	0.6764 (4)	0.3550 (6)	−0.2246 (4)	5 (1)
C(51)	0.7061 (4)	0.3522 (6)	−0.2738 (4)	4 (1)
O(52)	0.6754 (3)	0.3518 (5)	−0.3476 (3)	7 (1)
C(53)	0.5945 (4)	0.3610 (9)	−0.3879 (5)	9 (2)
C(54)	0.7389 (5)	0.3539 (7)	−0.0773 (4)	7 (2)
O(55)	0.8615 (3)	0.3701 (5)	−0.4108 (3)	7 (1)
C(56)	0.7851 (5)	0.3715 (9)	−0.4677 (5)	8 (2)
C(57)	1.0501 (4)	0.3557 (8)	−0.1436 (5)	7 (2)
N(201)	0.6513 (4)	0.1254 (7)	0.2269 (4)	7 (2)
O(201)	0.6082 (4)	0.1938 (5)	0.2118 (4)	9 (2)
O(202)	0.7151 (4)	0.1419 (7)	0.2334 (4)	11 (2)
O(203)	0.6314 (7)	0.0458 (6)	0.2295 (7)	20 (3)
O(1)W	0.6541 (4)	0.5323 (5)	0.2184 (5)	8 (1)
N(301)	1.0821 (4)	0.8233 (7)	0.0224 (5)	6 (2)
O(301)	1.0665 (4)	0.7964 (6)	0.0716 (4)	9 (2)
O(302)	1.1001 (5)	0.7603 (8)	−0.0061 (5)	12 (2)
O(303)	0.4198 (5)	0.4095 (7)	0.4919 (6)	12 (2)
N(101)	0.9898 (5)	0.1570 (7)	0.2922 (6)	9 (2)
O(101)	0.9436 (4)	0.1902 (4)	0.3118 (4)	8 (1)
O(102)	1.0545 (5)	0.177 (1)	0.3292 (5)	18 (3)
O(103)	0.9726 (9)	0.118 (1)	0.239 (1)	34 (6)

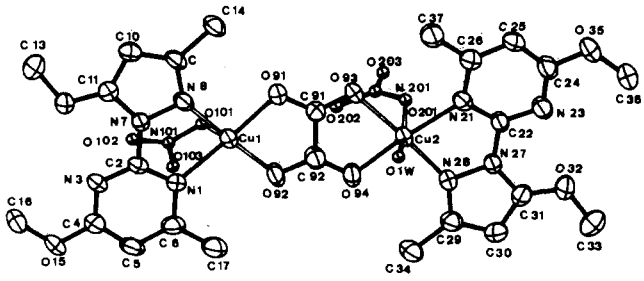

Figure 2. Projection of the noncentrosymmetric dimer **2A** onto its molecular plane.

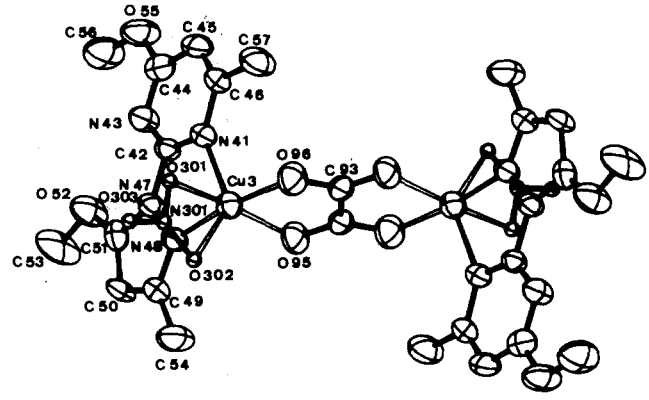

Figure 3. Projection of the centrosymmetric dimer **2B** onto a plane defined by Cu(3)···Cu(3)^{i} and N(41)···N(48). Hydrogen atoms are omitted, ellipsoids are scaled to enclose 50% probability. For clarity, NO_3^- ions and water molecules have been given arbitrary isotropic temperature factors.

anion is partially disordered: four of the six fluorine atoms statistically occupy two positions. By trial and error, the occupancy factors were estimated to be 70 and 30%. The P–F distances were constrained to the value of 1.58 Å. The phosphorus atom was refined anisotropically, but the fluorine atoms were kept isotropic. The oxygen atoms of the molecules of water of crystallization were also refined isotropically. When the least-squares refinements were carried out, the variable parameters were separated in two blocks, the first one referring to the complex ion and the second one to the uncoordinated ligand. The PF_6^- anions and the molecules of water of crystallization were refined in every cycle. The highest residual peaks of the final difference Fourier map are located in the region of the disordered PF_6^- anion, indicating that the model used in the refinement does not fully accommodate the distribution of the electronic density.

Final agreement factor values are given in Table I. Positional parameters and equivalent or isotropic temperature factors for non-hydrogen atoms are given in Table II; atoms are labeled according to Figure 1. Components of the anisotropic temperature factors, hydrogen atom positional parameters, and observed and calculated structure factors amplitudes are deposited as supplementary material. Bond lengths and angles are listed in Table III.

Complex 2. The refinement was conducted by using the full-matrix least-squares procedure. All non-hydrogen atoms were assigned anisotropic thermal parameters. All hydrogen atoms, including those of the water molecule, were located on difference Fourier maps and included in the calculations by using idealized positions (C–H = 0.97 Å and O–H = 0.80 Å) and arbitrary isotropic temperature factors (U = 0.07 Å^2). The NO_3^- anions are coordinated to the copper atoms but undergo a strong thermal motion. The NO_3^- ion bonded to the Cu(1) atom is likely to be disordered: the unusually large displacement parameters of the uncoordinated O(102) and O(103) atoms are physically meaningless and result from the refinement process, which tries to accommodate the electronic density spread over a large volume. This is indicative of an unresolved disorder. Furthermore, the largest residual peak of the final difference Fourier map (0.8 e Å^{-3}) is located 1.25 Å away from N(101), with a peak–N(101)–O(101) angle = 122°. However, no chemically significant model of disorder could be found to accommodate this residual electronic density. All other residual peaks are less than 0.5 e Å^{-3}.

Final agreement factor values are given in Table I. Positional parameters and equivalent isotropic temperature factors for non-hydrogen atoms are given in Table IV; atoms are labeled according to Figures 2 and 3. Components of the anisotropic temperature factors, hydrogen atom positional parameters, and observed and calculated structure factor amplitudes have been deposited as supplementary material. Bond lengths and angles are listed in Table V.

Physical Measurements. Infrared spectra were obtained as KBr pellets on a Perkin-Elmer 843 spectrophotometer. Electronic absorption spectra were recorded with a Perkin-Elmer Lambda 15 spectrophotometer.

Variable-temperature magnetic susceptibility data were obtained as previously described[17] on polycrystalline samples with a Faraday-type magnetometer equipped with a continuous-flow Oxford Instrument cryostat. Least-squares computer fittings of the magnetic susceptibility data were carried out with an adapted version of the function-minimization program STEPT.[18]

EPR spectra were obtained on a Bruker 200 TT spectrometer equipped as previously described.[19]

Results and Discussion

Synthesis. In attempts to grow single crystals of **4** the synthetic procedure described in the Experimental Section was followed, and the final green solution was filtered and allowed to stand at room temperature. Green-blue crystals formed within a few days. The analytical data for these crystals correspond to those previously obtained for complex **2**, and the powder X-ray diffraction pattern of the crystals is identical with that exhibited by complex **2** while the X-ray pattern of powder samples of **4** is different. In addition, the IR frequency observed at 3310 cm^{-1} in the powder of **4** corresponds to the N-H stretch and is lacking in the IR spectrum of the green-blue crystals (vide infra). These observations indicate that the attempts made to crystallize complex **4** resulted in hydrolysis of the oxamido bridge. This is consistent with previously mentioned results.[20]

Crystal Structure of 1. The structure consits of centrosymmetric binuclear cations $[L(H_2O)Cu(ox)Cu(H_2O)L]^{2+}$ separated by PF_6^- anions, free mepirizole molecules, and molecules of water of crystallization. The struture of the complex cation is shown in Figure 1. The two copper atoms are linked through a bis-bidentate oxalate group leading to a metal–metal separation of 5.175 Å.

The Cu(II) ions are in a 4 + 1 environment. The basal coordination positions are occupied by two oxalate oxygen atoms, O(18) and O(20), and two nitrogen atoms of the bidentate mepirizole ligand, N(1) and N(8). The corresponding Cu–O and Cu–N distances are of the same magnitude, ranging from 1.96 to 2.02 Å. The apical position is occupied by the oxygen atom of a water molecule at a larger distance (2.24 Å). As expected, the copper atom is 0.24 Å out of the basal plane toward the apex. The tetragonality parameter[21,22] of the coordination polyhedron of the copper atom (T = 0.89) is similar to that previously obtained for $[Cu_2(phen)_2(ox)(NO_3)_2]$[23] (phen = 1,10-phenanthroline), indicating a trend toward the square-planar arrangement, consistent with a weak interaction with the apical H_2O molecule. The distortion of the coordination polyhedron around the copper atom can be quantified by using the approach of Muetterties and Guggenberger.[24] In this method, the dihedral angles between adjacent faces (known as the shape-determining angles e_1, e_2, and e_3) are calculated in order to describe an intermediate geometry. The key shape-determining angle, e_3, is 0.0° for an ideal square pyramid (SP) and 53.1° for an ideal trigonal bipyramid (TBP).

(17) Luneau, D.; Savariault, J.-M.; Cassoux, P.; Tuchagues, J.-P. *J. Chem. Soc., Dalton Trans.* **1988**, 1225–1235.
(18) Chandler, J. P. Quantum Chemistry Program Exchange, Indiana University, Program 66.
(19) Mabad, B.; Cassoux, P.; Tuchagues, J.-P.; Hendrickson, D. N. *Inorg. Chem.* **1986**, *25*, 1420–1431.
(20) (a) Armendarez, P. X.; Nakamoto, K. *Inorg. Chem.* **1966**, *5*, 796–800 and references therein. (b) Verdaguer, M.; Kahn, O.; Julve, M.; Gleizes, A. *Nouv. J. Chim.* **1985**, *9*, 325–334.
(21) Procter, I. M.; Hathaway, B. J.; Nicholls, P. *J. Chem. Soc. A* **1968**, 1678–1684.
(22) Fitzgerald, W.; Foky, J.; McSweeney, D.; Ray, N.; Sheahan, D.; Tyagi, S.; Hathaway, B.; O'Brien, P. *J. Chem. Soc., Dalton Trans.* **1982**, 1117–1121.
(23) Bencini, A.; Fabretti, A. C.; Zanchini, C.; Zannini, P. *Inorg. Chem.* **1987**, *26*, 1445–1449.
(24) Muetterties, E. L.; Guggenberger, L. J. *J. Am. Chem. Soc.* **1974**, *96*, 1748–1756.

Table V. Selected Interatomic Distances (Å) and Bond Angles (deg) for Complex **2**[a]

Unit **2A**

Coordination Sphere [Cu(1)]

Cu(1)–O(91)	1.939 (4)	Cu(1)–O(101)	2.361 (6)	Cu(1)–O(92)	1.981 (6)	Cu(1)–N(8)	1.955 (4)
Cu(1)–N(1)	2.039 (7)						
O(91)–Cu(1)–O(92)	83.9 (2)	O(91)–Cu(1)–O(101)	88.9 (2)	O(92)–Cu(1)–O(101)	99.4 (3)	N(1)–Cu(1)–O(101)	86.8 (3)
O(91)–Cu(1)–N(1)	100.4 (2)	O(92)–Cu(1)–N(1)	172.7 (2)	N(1)–Cu(1)–N(8)	81.7 (3)	N(8)–Cu(1)–O(101)	95.2 (2)
O(91)–Cu(1)–N(8)	175.6 (3)	O(92)–Cu(1)–N(8)	93.6 (2)				

Coordination Sphere [Cu(2)]

Cu(2)–O(93)	1.971 (6)	Cu(2)–O(201)	2.541 (7)	Cu(2)–N(28)	1.964 (5)	Cu(2)–O(1)W	2.243 (7)
Cu(2)–N(21)	2.047 (7)	Cu(2)–O(94)	2.010 (4)				
O(93)–Cu(2)–O(94)	83.5 (2)	O(93)–Cu(2)–O(1)W	89.7 (3)	O(94)–Cu(2)–O(1)W	86.4 (2)	N(28)–Cu(2)–O(201)	90.1 (2)
O(93)–Cu(2)–N(21)	172.1 (2)	O(94)–Cu(2)–N(21)	103.5 (2)	N(21)–Cu(2)–N(28)	81.0 (2)	N(28)–Cu(2)–O(1)W	99.3 (3)
O(93)–Cu(2)–N(28)	91.7 (2)	O(94)–Cu(2)–N(28)	172.5 (3)	N(21)–Cu(2)–O(201)	82.6 (3)	O(201)–Cu(2)–O(1)W	169.8 (3)
O(93)–Cu(2)–O(201)	94.1 (3)	O(94)–Cu(2)–O(201)	84.6 (2)	N(21)–Cu(2)–O(1)W	94.4 (3)		

Oxalato Bridge

O(91)–C(91)	1.26 (1)	O(93)–C(91)	1.24 (1)	O(94)–C(92)	1.25 (1)	C(91)–C(92)	1.51 (1)
O(92)–C(92)	1.25 (1)						
O(91)–C(91)–O(93)	126.3 (8)	O(93)–C(91)–C(92)	117.8 (8)	O(92)–C(92)–C(91)	116.3 (7)	O(94)–C(92)–C(91)	116.5 (5)
O(91)–C(91)–C(92)	115.9 (5)	O(92)–C(92)–O(94)	127.1 (8)				

Mepirizole Molecules

N(1)–C(2)	1.31 (1)	C(4)–C(5)	1.37 (1)	N(7)–C(11)	1.36 (1)	C(10)–C(11)	1.37 (2)
N(1)–C(6)	1.37 (1)	C(4)–O(15)	1.33 (1)	N(8)–C(9)	1.33 (1)	C(11)–O(12)	1.33 (1)
C(2)–N(3)	1.32 (1)	C(5)–C(6)	1.37 (1)	C(9)–C(10)	1.38 (1)	O(12)–C(13)	1.44 (1)
C(2)–N(7)	1.41 (1)	C(6)–C(17)	1.47 (1)	C(9)–C(14)	1.50 (1)	O(15)–C(16)	1.44 (1)
N(3)–C(4)	1.31 (1)	N(7)–N(8)	1.39 (1)				
C(2)–N(1)–C(6)	115.2 (7)	C(5)–C(4)–O(15)	118.1 (8)	C(2)–N(7)–C(11)	132.5 (7)	C(9)–C(10)–C(11)	105.8 (6)
N(1)–C(2)–N(3)	129.3 (7)	C(4)–C(5)–C(6)	118.5 (8)	N(8)–N(7)–N(11)	110.1 (6)	N(7)–C(11)–C(10)	107.5 (6)
N(1)–C(2)–N(7)	115.5 (7)	N(1)–C(6)–C(5)	119.6 (6)	N(7)–N(8)–C(9)	104.5 (5)	N(7)–C(11)–O(12)	120.5 (7)
N(3)–C(2)–N(7)	115.2 (5)	N(1)–C(6)–C(17)	119.1 (8)	N(8)–C(9)–C(10)	112.2 (8)	C(10)–C(11)–O(12)	132.0 (5)
C(2)–N(3)–C(4)	114.7 (5)	C(5)–C(6)–C(17)	121.3 (8)	N(8)–C(9)–C(14)	121.7 (6)	C(11)–O(12)–C(13)	114.5 (7)
N(3)–C(4)–C(5)	122.7 (8)	C(2)–N(7)–N(8)	117.6 (5)	C(10)–C(9)–C(14)	126.1 (7)	C(4)–O(15)–O(16)	117.6 (7)
N(3)–C(4)–O(15)	119.2 (5)						
N(21)–C(22)	1.33 (1)	C(24)–C(25)	1.35 (1)	N(27)–C(31)	1.37 (1)	C(30)–C(31)	1.38 (1)
N(21)–C(26)	1.36 (1)	C(24)–O(35)	1.35 (1)	N(28)–C(29)	1.34 (1)	C(31)–O(32)	1.31 (1)
C(22)–N(23)	1.33 (1)	C(25)–C(26)	1.38 (1)	C(29)–C(30)	1.39 (1)	O(32)–C(33)	1.43 (1)
C(22)–N(27)	1.40 (1)	C(26)–C(37)	1.47 (1)	C(29)–C(34)	1.50 (1)	O(35)–C(36)	1.42 (1)
N(23)–C(24)	1.32 (1)	N(27)–N(28)	1.39 (1)				
C(22)–N(21)–C(26)	114.7 (6)	C(25)–C(24)–O(35)	118.2 (9)	C(22)–N(27)–C(31)	132.4 (6)	C(30)–C(29)–C(34)	126.1 (7)
N(21)–C(22)–N(23)	129.1 (8)	C(24)–C(25)–C(26)	118.1 (6)	N(28)–N(27)–C(31)	110.2 (7)	C(29)–C(30)–C(31)	105.6 (7)
N(21)–C(22)–N(27)	115.5 (7)	N(21)–C(26)–C(25)	120.2 (6)	C(22)–N(27)–N(28)	117.1 (3)	N(27)–C(31)–C(30)	107.3 (6)
N(23)–C(22)–N(27)	115.4 (5)	N(21)–C(26)–C(37)	118.5 (7)	N(27)–N(28)–C(29)	104.7 (5)	N(27)–C(31)–O(32)	120.0 (8)
C(22)–N(23)–C(24)	113.7 (5)	C(25)–C(26)–C(37)	121.2 (8)	N(28)–C(29)–C(30)	112.1 (8)	C(30)–C(31)–O(32)	132.7 (5)
N(23)–C(24)–C(25)	124.3 (8)	C(31)–O(32)–C(33)	115.1 (7)	N(28)–C(29)–C(34)	121.8 (5)	C(24)–O(35)–C(36)	119.4 (7)
N(23)–C(24)–O(35)	117.5 (6)						

Nitrate Ions

N(101)–O(101)	1.26 (1)	N(101)–O(102)	1.17 (1)	N(101)–O(103)	1.09 (2)
O(101)–N(101)–O(102)	118 (1)	O(101)–N(101)–O(103)	124 (1)	O(102)–N(101)–O(103)	118 (2)
N(201)–O(201)	1.22 (1)	N(201)–O(202)	1.24 (1)	N(201)–O(203)	1.18 (1)
O(201)–N(201)–O(202)	117 (1)	O(201)–N(201)–O(203)	121 (1)	O(202)–N(201)–O(203)	121 (1)

Unit **2B**

Coordination Sphere [Cu(3)]

Cu(3)–O(95)	2.057 (6)	Cu(3)–N(41)	2.201 (7)	Cu(3)–O(301)	2.111 (8)	Cu(3)–O(302)	2.44 (1)
Cu(3)–O(96)	1.961 (5)	Cu(3)–N(48)	1.966 (5)				
O(95)–Cu(3)–O(96)	81.6 (2)	O(95)–Cu(3)–O(302)	117.5 (3)	O(96)–Cu(3)–O(302)	89.9 (3)	N(48)–Cu(3)–O(301)	97.1 (2)
O(95)–Cu(3)–N(41)	101.6 (2)	O(96)–Cu(3)–N(41)	105.9 (3)	N(41)–Cu(3)–N(48)	77.5 (3)	N(48)–Cu(3)–O(302)	92.6 (3)
O(95)–Cu(3)–N(48)	89.7 (2)	O(96)–Cu(3)–N(48)	171.1 (3)	N(41)–Cu(3)–O(301)	89.5 (3)	O(301)–Cu(3)–O(302)	52.6 (4)
O(95)–Cu(3)–O(301)	168.1 (2)	O(96)–Cu(3)–O(301)	91.2 (2)	N(41)–Cu(3)–O(302)	139.6 (3)		

Oxalato Bridge

O(95)–C(93)	1.24 (1)	C(93)–C(93)^{i}	1.49 (1)	C(93)–O(96)	1.26 (3)
O(95)–C(93)–O(96)	126.1 (2)	C(93)^{i}–C(93)–O(96)	115.5 (5)	O(95)–C(93)–C(93)^{i}	118.4 (3)

Mepirizole

N(41)–C(42)	1.32 (1)	C(44)–C(45)	1.38 (1)	N(47)–C(51)	1.38 (1)	C(50)–C(51)	1.38 (1)
N(41)–C(46)	1.37 (1)	C(44)–O(55)	1.35 (1)	N(48)–C(49)	1.33 (1)	C(51)–O(52)	1.29 (1)
C(42)–N(43)	1.33 (1)	C(45)–C(46)	1.35 (1)	C(49)–C(50)	1.39 (1)	O(52)–C(53)	1.43 (1)
C(42)–N(47)	1.41 (1)	C(46)–C(57)	1.49 (1)	C(49)–C(54)	1.49 (1)	O(55)–C(56)	1.40 (1)
N(43)–C(44)	1.30 (1)	N(47)–N(48)	1.38 (1)				

Table V (Continued)

C(42)-N(41)-C(46)	114.0 (6)	C(45)-C(44)-O(55)	117.9 (8)	C(42)-N(47)-C(51)	132.4 (6)	C(49)-C(50)-C(51)	105.6 (7)
N(41)-C(42)-N(43)	130.3 (8)	C(44)-C(45)-C(46)	118.7 (8)	N(48)-N(47)-C(51)	109.4 (7)	N(47)-C(51)-C(50)	107.3 (6)
N(41)-C(42)-N(47)	114.9 (7)	N(41)-C(46)-C(45)	120.4 (6)	N(47)-N(48)-C(49)	106.2 (5)	N(47)-C(51)-O(52)	119.5 (8)
N(43)-C(42)-N(47)	114.8 (5)	N(41)-C(46)-C(57)	116.4 (7)	N(48)-C(49)-C(50)	111.5 (8)	C(50)-C(51)-O(52)	133.3 (7)
C(42)-N(43)-C(44)	113.4 (6)	C(45)-C(46)-C(57)	123.2 (8)	N(48)-C(49)-C(54)	120.9 (6)	C(51)-O(52)-C(53)	115.2 (8)
N(43)-C(44)-C(45)	123.3 (8)	C(42)-N(47)-N(48)	117.8 (5)	C(50)-C(49)-C(54)	127.6 (8)	C(44)-O(55)-C(56)	118.6 (8)
N(43)-C(44)-O(55)	118.9 (6)						

Nitrate Ion

N(301)-O(301)	1.23 (1)	N(301)-O(302)	1.19 (1)	N(301)-O(303)	1.22 (1)
O(301)-N(301)-O(302)	115 (1)	O(301)-N(301)-O(303)	120 (1)	O(302)-N(301)-O(303)	126 (1)

[a] Superscript i indicates an inversion through a center of symmetry.

For the considered compound, $e_3 = 8.2°$, indicating a strong predominance of the SP form. This coordination polyhedron is very different from the one described in a previous paper[7c] for the corresponding monomer CuL(ox)(H_2O). In the latter, the five-coordination polyhedron is intermediate between the SP and TBP forms. Moreover, the water molecule lies closer to the Cu atom (1.966 Å) while the Cu-N(8) distance is 2.174 Å.

Interatomic distances and bond angles in the mepirizole and oxalate moieties are in good agreement with previously reported data.[7b,c] The mepirizole ligand is almost planar: the torsional angle N(1)-C(2)-N(7)-N(8) is 2.5° and the dihedral angle between the pyrazole and the pyrimidine rings is 3.4° (deviations from the least-squares planes are given as supplementary material). The binuclear complex ion is folded as indicated in Figure 4a: the basal coordination plane makes an angle $\alpha = 162.0°$ with the mean plane of the oxalato ligand. In addition, the angle between this coordination plane and the mean plane of the mepirizole ligand is 166°. As a result, the binuclear complex displays the stairlike structure.[9] However, because of the out-of-plane position of the copper atoms, the central Cu(ox)Cu core is nearly planar: the largest deviation from the mean plane is ±0.04 Å for the O(20) atoms.

The complex cations form layers parallel to (010) at the mean levels $y = 0$ and $y = {}^1/_2$. The mean plane of the coordinated mepirizole molecule is almost parallel to (010). These layers alternate with layers of strictly planar free mepirizole molecules lying in the crystallographic mirror parallel to (010) at the levels $y = {}^1/_4$ and $y = {}^3/_4$. The PF_6^- anions and the molecules of water of crystallization are located between the layers.[9] Hydrogen bonds are likely to occur between the molecules of water of crystallization and coordinated water molecules: O(2)w···O(1)w = 2.94 Å, O(3)w···O(1)w = 2.83 Å.

Crystal Structure of 2. The structure is built up of two crystallographically independent dimers [L(NO_3)Cu(ox)Cu(NO_3)(H_2O)L] and [L(NO_3)Cu(ox)Cu(NO_3)L] (the latter is centrosymmetric) hereafter referred to as units **2A** and **2B**. The structures are drawn in Figures 2 and 3. In both units, the bisbidentate oxalate group links the two copper atoms forming five-membered chelate rings. The Cu···Cu separations are 5.149 (1) and 5.268 (1) Å for units **2A** and **2B**, respectively. The ability of the copper atom to achieve various coordination geometries has been illustrated by a number of examples, leading to the concept of "plasticity" proposed by Hathaway.[25] Complex **2** once again illustrates this concept: each of the three crystallographically independent copper atoms lies in a different environment.

The coordination of the Cu(1) atom can be described as the 4 + 1 SP-type similar to that of complex **1**. The basal coordination positions are occupied by two oxalate oxygen atoms, O(91) and O(92), and two nitrogen atoms from the bidentate mepirizole ligand, N(1) and N(8). The Cu-O and Cu-N distances range from 1.94 to 2.04 Å. The apex is occupied by an oxygen atom from a monodentate NO_3^- ion at a larger distance (2.36 Å). The copper atom is only 0.08 Å out of the basal plane toward the apex. The tetragonality parameter ($T = 0.84$) indicates a strong tendency to square-planar arrangement consistent with a weak interaction with the apical NO_3^- ion. The value of $e_3 = 1.48°$, determined in accordance with Muetterties' method,[24] is consistent with a strong predominence of the SP geometry over the TBP one.

The coordination of the Cu(2) atom would be best described as a 4 + 2 distorted octahedral. The equatorial plane involves the oxalate oxygen atoms, O(93) and O(94), and the mepirizole nitrogen atoms, N(21) and N(28), with Cu-O and Cu-N distances ranging from 1.96 to 2.04 Å. The apical positions are occupied by a water molecule, Cu-O(1)w = 2.26 Å, and an oxygen atom from a NO_3^- anion, Cu-O(201) = 2.54 Å. As a consequence, the copper atom is pulled 0.08 Å out of the equatorial plane toward the O(1)w water molecule.

As usually observed, the mepirizole ligand is close to planarity in each moiety of this dimer: the relevant torsional angles are N(1)-C(2)-N(7)-N(8) = -3.3° and N(21)-C(22)-N(27)-N(28) = -0.6°, and the corresponding dihedral angles between the pyrazole and the pyrimidine rings are 4.5 and 5.1°, respectively (deviations of atoms from the least-squares planes are given as supplementary material). As a whole (apical groups omitted), dimer **2A** is close to planarity. The angles between the mean plane of the oxalato bridge and the mean coordination planes are $\alpha = 166°$ and $\beta = 178°$ (Figure 4b). However, the central Cu(ox)Cu core is not planar: the Cu(1) and Cu(2) atoms deviate from the Cu(ox)Cu mean plane by 0.16 and 0.13 Å, respectively, and from the oxalate mean plane by 0.26 and 0.13 Å, respectively. A side view of unit **2A** is provided as supplementary material.

Unit **2B** (Figure 3) is centrosymmetric with a center of symmetry lying in the middle of the C-C bond of the bis-bidentate oxalate bridge. The Cu(3)-O(95) and Cu(3)-O(96) distances (2.06 and 1.96 Å, respectively) are in the usual range. As previously observed, the mepirizole ligand is bonded through N(41) and N(48) atoms. However, while the Cu(3)-N(48) distance (1.97 Å) is normal, the Cu(3)-N(41) distance (2.20 Å) is rather large. The N(41) atom has been pushed away from the Cu(3) atom to allow a nitrate ion to enter the coordination sphere in a bidentate mode. However, the Cu-O distances are quite different (Cu(3)-O(301) = 2.11 Å, and Cu(3)-O(302) = 2.44 Å) and the corresponding O-Cu-O angle is quite acute (52.6°). As a result, the coordination polyhedron of the Cu(3) atom can barely be considered as an octahedron. It is however possible to define an equatorial plane involving O(301), N(48), O(95), and O(96), i.e. the closest atoms to Cu(3). Deviations of atoms from this plane are +0.046, +0.026, +0.007, and -0.079 Å, respectively. Furthermore, the angles about the Cu(3) atom do not deviate too much from 90°. Thus, the main distortion from the octahedral geometry arises from the axial O(302)-Cu(3)-N(41) angle (139.6°). The central part of this complex unit is close to planarity: the folding angle is $\alpha = 177°$ (Figure 4a). The Cu(ox)Cu core is also almost planar (maximum deviation: ±0.048 Å for O(96)). As usual, the mepirizole ligand does not deviate too much from planarity: the key torsional angle N(41)-C(42)-N(47)-N(48) is 2.8°, and the dihedral angle between the pyrazole and the pyrimidine rings is 3.9° (deviations of atoms from the least-squares planes are given as supplementary material). However, the plane of the terminal ligand is almost perpendicular to the plane of the bridge (dihedral angle = 99°).

Electronic Properties. The diffuse reflectance spectra of compounds **1** and **3** are compatible with the presence of the chro-

(25) Hathaway, B. J. *Struct. Bonding* **1984**, *57*, 55-118.

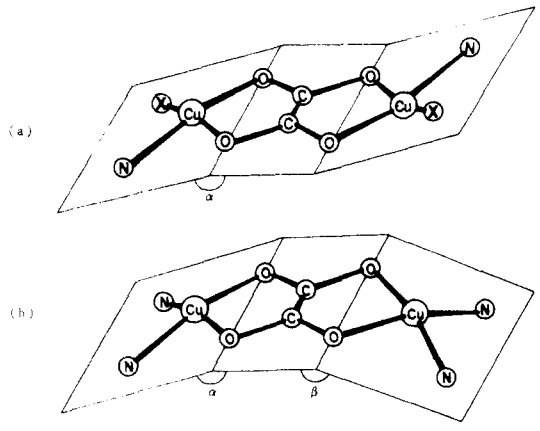

Figure 4. Schematic view of the central part of the binuclear units showing the dihedral angles between the copper coordination planes and the oxalato bridge. (a) centrosymmetric units: complex **1**, $\alpha = 162°$; complex **2B**, $\alpha = 177°$; (b) noncentrosymmetric unit: complex **2A**, $\alpha = 166°$, $\beta = 178°$.

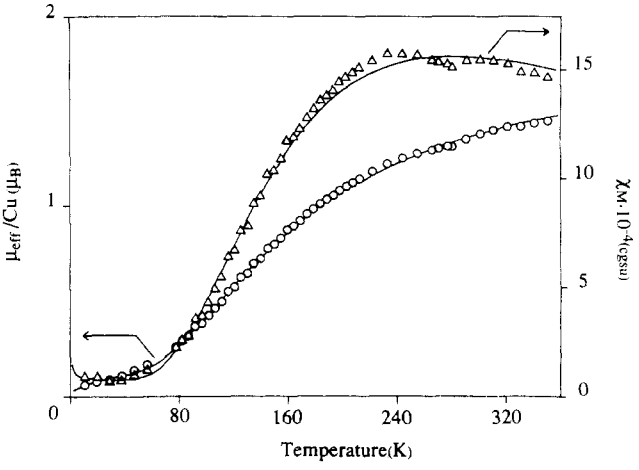

Figure 5. Experimental molar magnetic susceptibility per dimer (Δ) and effective magnetic moment per Cu(II) ion (O) vs temperature for **2**. The solid lines represent the least-squares fit to eq 1.

mophore CuN_2O_2O' (where the two "O" oxygen atoms originate from $C_2O_4^{2-}$ and the "O'" originates from H_2O or ClO_4^- groups).

The maximum observed for compound **1** (d–d band at 14 300 cm^{-1}) is consistent with the SP geometry[26] and agrees with the results obtained in the X-ray study. The geometry is presumably similar for complex **3** (d–d band at 14 600 cm^{-1}).

The three coordination sites in compound **2** lead to three different chromophores: two of them are roughly octahedral ($Cu(1)N_2O_2O'O''$ and $Cu(3)N_2O_2O'_2$) and one is square pyramidal ($Cu(2)N_2O_2O'$). Thus, the visible spectrum observed for this compound (d–d band at 12 500 cm^{-1}) will be the result of overlapping of bands generated by the d–d transition characteristic of each chromophore and consequently cannot be easily interpreted.

Finally, the spectrum of compound **4** (d–d band at 13 600 cm^{-1}) is compatible with the existence of a pentacoordinated Cu(II) ion (chromophore CuN_3OO').

IR Spectroscopy. The IR spectrum of complex **4** shows an absorption frequency at 3310 cm^{-1} assigned to the ν_{N-H} stretching frequency. The oxalato and oxamido groups exhibit infrared absorption frequencies assignable to a bis-bidentate bridging mode.[27]

The IR spectrum of compound **1** indicates that the counteranion PF_6^- is not coordinated. Concerning complexes 2–4, the absorption frequencies assigned to the ClO_4^- and NO_3^- groups indicate coordination to the metal ion.

Magnetic Properties. The room-temperature magnetic moments of complexes **1–4** are all below the value expected for single copper(II) ions, showing the presence of antiferromagnetic coupling. The magnetic susceptibility of **1–4** has been measured in the 360–5 K temperature range, affording the data compiled in the supplementary material and displayed in Figure 5 for complex **2** and in the supplementary material for **1**, **3**, and **4**.

The singlet–triplet energy gap ($2J$) was deduced from the least-squares fit of the experimental data to the temperature dependence of the molar magnetic susceptibility χ_M expressed according to the Bleaney–Bowers equation for isotropic exchange in a Cu(II) dimer.[28] This equation has been modified to take into account admixture of paramagnetic impurity, according to ref 29:

$$\chi_M = [(2N\beta^2g^2)/(kT)][3 + \exp(-(2J)/(kT))]^{-1}(1 - \rho) + (N\beta^2g^2)(2kT)^{-1}\rho + 2N\alpha \quad (1)$$

where the symbols have their usual meaning and ρ is the percent of noncoupled impurity, the molecular weight of which is assumed to be equal to that of the binuclear complex.

Since the diamagnetic correction is of the same order of magnitude as the uncorrected molar susceptibility, the uncertainty on the corrected values of χ_M is large, affording estimated J values reliable only within 5–10%.[30]

The calculated J, g, ρ and $2N\alpha$ values are given in Table VI, together with the agreement factor R defined as

$$R = \{\sum_{i=1}^{NP}[\mu_{eff}(obsd)_i - \mu_{eff}(calcd)_i]^2/(NP - k)\}^{1/2}$$

where k is the number of variable parameters used to fit the NP data points.[31]

The results, gathered in Table VI, indicate that **1** exhibits the larger antiferromagnetic intramolecular interaction. This observation can be rationalized on the basis of the theory developed by Kahn et al.[3,32]

The previously described centrosymmetric structure of **1** is characterized by a square-pyramidal coordination geometry around each Cu(II) ion of the binuclear unit. In this 4 + 1 environment, the Cu(II) unpaired electron is described by a d_{xy} type orbital pointing from the metal toward the four nearest neighbors in an antibonding fashion.[3,32] Since the trigonal-bipyramidal character of this 4 + 1 coordination of the Cu(II) is very small, the spin density onto the farthest O(1)w ligand should be negligible. This coordination geometry is the most favorable to achieve a strong antiferromagnetic interaction through the oxalato bridge since the magnitude of the antiferromagnetic contribution (J_{AF}), related to the square of the overlap between the magnetic orbitals centered on each Cu(II) ion, is essentially governed by their delocalization onto the oxygen atoms of the oxalato bridge.[33] Furthermore, the ferromagnetic contribution (J_F) has been shown to be weak when the metal centers are bridged by polyatomic extended ligands as oxalato anions.[34,35]

The −201 cm^{-1} exchange integral, J, calculated for **1**, compares well with the −193 cm^{-1} values obtained for the structurally similar $[(tmen)(H_2O)Cu(ox)Cu(H_2O)(tmen)](ClO_4)_2 \cdot 1.25H_2O$[33] (tmen = 1,1,4,4-tetramethylethylenediamine) and $[Cu_2(bpy)_2(H_2O)_2(ox)][Cu(bpy)(ox)](NO_3)_2$[36] (bpy = 2,2'-bipyridyl), the difference being within the estimated error range. However, the [Cu_2-

(26) Lever, A. B. P. *Inorganic Electronic Spectroscopy*, 2nd ed.; Elsevier: Amsterdam, The Netherlands, 1986.
(27) Nakamoto, R. *Infrared and Raman Spectra of Inorganic and Coordination Compounds*, 4th ed.; Wiley: New York, 1986.
(28) Bleaney, B.; Bowers, K. D. *Proc. R. Soc. London, A* **1952**, *214*, 451–465.
(29) Journaux, Y.; Sletten, J.; Kahn, O. *Inorg. Chem.* **1985**, *24*, 4063–4069.
(30) O'Connor, C. *Prog. Inorg. Chem.* **1982**, *20*, 203–283.
(31) Ginsberg, A. P.; Martin, R. L.; Brookes, R. W.; Sherwood, R. C. *Inorg. Chem.* **1972**, *11*, 2884–2889.
(32) (a) Kahn, O.; Charlot, M. F. *Nouv. J. Chim.* **1980**, *10*, 567–570. (b) Kahn, O. *Inorg. Chim. Acta* **1982**, *62*, 3–14.
(33) Julve, M.; Verdaguer, M.; Kahn, O.; Gleizes, A.; Philoche-Levisalles, M. *Inorg. Chem.* **1983**, *22*, 368–370.
(34) Julve, M.; Verdaguer, M.; Gleizes, A.; Philoche-Levisalles, M.; Kahn, O. *Inorg. Chem.* **1984**, *23*, 3808–3818.
(35) Julve, M.; Verdaguer, M.; Charlot, M. F.; Kahn, O.; Claude, R. *Inorg. Chim. Acta* **1984**, *82*, 5–12.
(36) Julve, M.; Faus, J.; Verdaguer, M.; Gleizes, A. *J. Am. Chem. Soc.* **1984**, *106*, 8306–8308.

Table VI. Summary of Magnetic Susceptibility and EPR Parameters for Complexes **1**–**4**

complex	J, cm^{-1}	ρ, %	$10^5(2N\alpha)$	g^a	10^2R	$g_{av}{}^b$	A, G
$[Cu_2L_2(ox)(H_2O)_2](PF_6)_2\cdot L\cdot 3H_2O$ (**1**)	−201	0.5	6	2.18	1.8	2.16, 4.2	85
$[Cu_2L_2(ox)(NO_3)_2(H_2O)]_2$							
$[Cu_2L_2(ox)(NO_3)_2]$ (**2**)	−156	4×10^{-4}	8	2.12	1.3	2.14, 4.2	70
$[Cu_2L_2(ox)(ClO_4)_2]$ (**3**)	−175	0	0	2.20	1.4	2.17, 4.2	75
$[Cu_2L_2(oxa)(NO_3)_2]\cdot H_2O$ (**4**)	−195	0	4	1.97	1.9	2.17, 4.2	80

[a] From magnetic susceptibility fitting. [b] Average g values from X-band EPR spectra at 130 K.

$(phen)_2(ox)(NO_3)_2]$ complex, although being structurally similar,[23] exhibits a weaker antiferromagnetic interaction.[37]

Among the four complexes studied herein, **2** exhibits the weaker antiferromagnetic interaction, $J = -156$ cm^{-1}. As described in the crystal structure section, **2** is built up from two crystallographically independent binuclear units, **2A** and **2B**, in the relative proportion of $^2/_3$ to $^1/_3$, respectively.

In unit **2A**, the coordination geometry around Cu(1) is square pyramidal (4 + 1 type) while the coordination geometry around Cu(2) is distorted octahedral (4 + 2 type). The Cu–oxalato–Cu core has a boat conformation. Again, the copper(II) unpaired electron will be described by a d_{xy} type orbital pointing from the metal toward the four nearest neighbors in an antibonding fashion in both types (4 + 1 and 4 + 2) of environments.

However, as recalled above, unit **2A** is not symmetrical. Kahn et al.[38] have established that for a symmetrical Cu(II) binuclear complex such as **1**, the antiferromagnetic contribution J_{AF} to the exchange interaction may be expressed as $J_{AF} = -2S\Delta$, S being the overlap integral between the magnetic orbitals centered on the two transition ions and Δ being the energy separation betwen the two singly occupied molecular orbitals in the triplet state built from the magnetic orbitals. When the geometry of the ligand environment of the Cu(II) ions of the binuclear complex is not strictly identical (which is the case for unit **2A**), the binuclear complex is not symmetrical and the antiferromagnetic contribution must be expressed according to $J_{AF} = -2S(\Delta^2 - \delta^2)^{1/2}$, δ being the energy separation between the two magnetic orbitals.[39] The δ value and the corresponding decrease of the antiferromagnetic contribution J_{AF} that result from the lowering of the symmetry have been calculated by Girerd et al.[40] in the case of dithiooxamidato binuclear copper(II) complexes. The authors have shown that the decrease in J_{AF} estimated from extended Hückel MO calculations is in good agreement with that estimated from the magnetic susceptibility measurements. We can thus anticipate that the antiferromagnetic interaction afforded by the coordination geometry of unit **2A** will be weaker than that achieved through the symmetrical coordination geometry of complex **1**.

In the centrosymmetric unit **2B**, the coordination geometry around each copper(II) ion is distorted octahedaral (4 + 2 type). The Cu–oxalato–Cu core is almost planar with a flattened chair conformation. The copper(II) unpaired electron is described by a d_{xy} orbital and the coordination geometry of unit **2B** is favorable to achieve a strong antiferromagnetic interaction through the oxalato bridge.

The bulk magnetic susceptibility measurements obtained for **2** allow one to obtain the average value of the magnetic interactions operating in both types of binuclear units, **2A** and **2B**. On the basis of the sensible hypothesis that the antiferromagnetic interaction operating in unit **2B** is similar to that calculated for complex **1**, it is possible to evaluate the antiferromagnetic interaction present in unit **2A** from the relation $J(\mathbf{2}) = 2J(\mathbf{2A})/3 + J(\mathbf{2b})/3$, which affords $J(\mathbf{2A}) = -133$ cm^{-1}. The conclusion of this rough evaluation would be that the previously described difference in the ligand environment of the Cu(II) ions of unit **2A** is able to induce an energy separation between the two magnetic orbitals large enough to weaken the antiferromagnetic interaction by approximately one-third.

The antiferromagnetic interaction calculated for complex **3** is weaker than those obtained for **1**, $[(tmen)(H_2O)Cu(ox)Cu(H_2O)(tmen)](ClO_4)_2\cdot 1.25H_2O$,[33] and $[Cu_2(bpy)_2(H_2O)_2(ox)][Cu(bpy)(ox)(NO_3)_2]$[36] and slightly larger than that obtained for $[Cu_2(phen)_2(ox)(NO_3)_2]$,[37] which points to some structural similarities between the latter complex and **3**. Unfortunately, the crystals of **3** we have obtained were not of good enough quality to carry out a single-crystal X-ray diffraction structure determination.

Finally, the −195-cm^{-1} exchange integral evaluated for the μ-oxamido-bridged complex **4** is the weakest among those evaluated for other oxamido-bridged copper(II) binuclear complexes, namely, −290 cm^{-1} for $\{[Cu(tmen)(H_2O)]_2oxamd\}(PF_6)_2$,[20b] −275 cm^{-1} for $[Cu_2oxa](BPh_4)_2\cdot 2(CH_3)_2CO$ (oxa = bis(6-ethyl-3,6-diazaoctyl)oxamido),[37,41] −265 cm^{-1} for $[Cu_2(phen)_2oxamd](NO_3)_2\cdot 1.5H_2O$,[37] −240 cm^{-1} for $[Cu_2(dpa)_2oxamd](NO_3)_2$,[37] and −220 cm^{-1} for $[Cu_2(oxpn)Cu(bpy)](ClO_4)_2$ (oxpn = *N*,*N*′-bis(3-aminopropyl)oxamido).[29] It is interesting to note that the latter complex for which the weaker antiferromagnetic interaction has been determined is nonsymmetrical and characterized by the presence of copper(II) ligand environments that are quite different (N_4 basal plane and 2.89 Å large Cu–O apical bond for Cu(1) vs N_2O_2 basal plane and 2.48 Å large Cu–O apical bond for Cu(2)). It seems logical to conclude that the weaker antiferromagnetic interaction observed for this complex arises from the energy separation between the two magnetic orbitals that results from the differences in the ligand environment of the two copper(II) ions. On these grounds, the weak antiferromagnetic interaction evaluated for the μ-oxamido-bridged complex **4** would lead to the hypothesis of a very disymmetrical ligand environment for the two Cu(II) ions of this compound.

EPR Spectroscopy. The room-temperature X-band powder EPR spectra of complexes **1**–**4** display broad resonances centered at ca. 3300 and 1600 G, corresponding to $\Delta M = \pm 1$ and $\Delta M = \pm 2$ transitions, respectively. Lowering the temperature of the samples to 100 K results in better resolved spectra, although the intensity of the resonances diminishes with temperature. These comments hold also for the Q-band spectra except that the $\Delta M = \pm 2$ transition is not detectable. Such spectra are associated with weakly anisotropic triplet states and very small zero-field splittings.[29,37,42,43]

Figure 6 displays X-band spectra of complex **1** at room temperature and 130 K. The half-field signal shows a seven-line hyperfine splitting, as expected for two equivalent copper(II) ions. The averaged hyperfine spacing, A, is 85 G, in agreement with the presence of exchange coupled Cu(II) ions.[42,44] Severe overlap of the individual lines in the $\Delta M = \pm 1$ region does not allow one to extract the principal components of the **g** tensor or to evaluate the zero-field splitting parameter D that must be smaller than the line width (0.03 cm^{-1}). On decreasing the temperature to 4.2 K, the EPR signals vanish, in accordance with strong antiferromagnetic coupling.

(37) Bencini, A.; Benelli, C.; Gatteschi, D.; Zanchini, C.; Fabretti, A. C.; Franchini, G. C. *Inorg. Chim. Acta* **1984**, *86*, 169–172.
(38) (a) Kahn, O.; Briat, B. *J. Chem. Soc., Faraday Trans. 2* **1976**, *72*, 268–281, 1441–1446. (b) Girerd, J.-J.; Charlot, M. F.; Kahn, O. *Mol. Phys.* **1977**, *34*, 1063–1076.
(39) Tola, P.; Kahn, O.; Chauvel, C.; Coudanne, H. *Nouv. J. Chim.* **1977**, *1*, 467–473.
(40) (a) Girerd, J.-J.; Jeannin, S.; Jeannin, Y.; Kahn, O. *Inorg. Chem.* **1978**, *17*, 3034–3040. (b) Chauvel, C.; Girerd, J.-J.; Jeannin, Y.; Kahn, O.; Lavigne, G. *Inorg. Chem.* **1979**, *18*, 3015–3020.
(41) Bencini, A.; Di Vaira, M.; Fabretti, A. C.; Gatteschi, D.; Zanchini, C. *Inorg. Chem.* **1984**, *23*, 1620–1623.
(42) Felthouse, T. R.; Laskowski, E. J.; Hendrickson, D. N. *Inorg. Chem.* **1977**, *16*, 1077–1089.
(43) Sonnenfroh, D.; Kreilick, R. W. *Inorg. Chem.* **1980**, *19*, 1259–1262.
(44) Slichter, C. P. *Phys. Rev.* **1955**, *99*, 479–480.

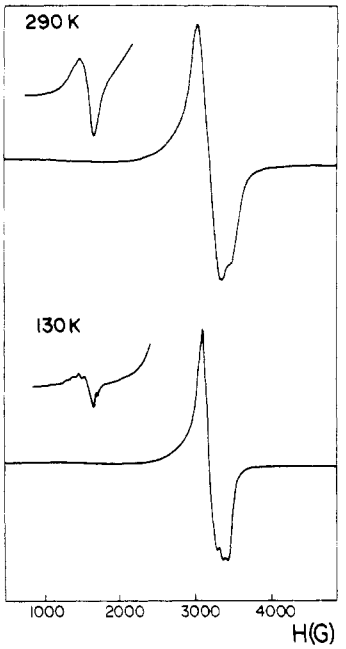

Figure 6. X-Band powder EPR spectra of complex **1** (microwave power 31 mW, microwave frequency 9.427 GHz, 10-G modulation amplitude).

The EPR spectra of complexes **2–4** are similar to those of **1**. The resulting EPR parameters are listed in Table VI.

Concluding Remarks

The study of four dimeric copper(II) complexes displaying large antiferromagnetic exchange interactions has been reported. The large exchange integrals arise from the important overlap of the d_{xy} magnetic orbitals which are coplanar with the oxalato or oxamido bridge.

Complex **1** is the first mepirizole compound that crystallizes with a molecule of free ligand. The structure of complex **2** is very unusual: it is built up from two crystallographically independent dimers in which the same ligands are involved with a different stereochemistry around the Cu(II) ions. On the basis of the sensible hypothesis that the antiferromagnetic interaction operating between the Cu(II) ions of unit **2B** is similar to that calculated for complex **1**, the magnitude of the antiferromagnetic interaction operating between the Cu(II) ions of unit **2A** has been evaluated.

Acknowledgment. We thank Dr. J. Galy for his constant interest in this work. We are grateful to Dr. J. V. Folgado for his friendly help. L.S. acknowledges the CNRS for permission to carry out part of this research at the Laboratoire de Chimie de Coordination, Toulouse, France, and the Generalitat Valenciana, Conselleria de Cultura, Educacio i Ciencia of Valencia, Spain, and the CAICYT (932/84) for financial assistance.

Registry No. **1**, 121886-87-1; **2**, 121865-93-8; **3**, 105236-60-0; **4**, 121865-94-9.

Supplementary Material Available: Figures 7–9, showing a side view of the $[Cu_2L_2(ox)(H_2O)_2]^{2+}$ cation of **1** (tilted by 10°), a partial representation of the crystal packing of **1** (projection onto (010)) and a side view of unit **2A** of complex **2**, respectively, Figures 10–12, showing the experimental and calculated molar magnetic susceptibility per dimer and effective magnetic moment per Cu(II) ion vs temperature for **1**, **3**, and **4**, respectively, Tables VII–IX, XI, XII, and XIV, listing crystallographic data, hydrogen atom positional parameters, final non-hydrogen atom thermal parameters, and deviations of atoms from least-squares planes for complexes **1** and **2**, respectively, and Tables XV–XVIII, listing the experimental magnetic susceptibility data for complexes **1–4**, respectively (23 pages); Tables X and XIII, listing the observed and calculated structure factor amplitudes for complexes **1** and **2**, respectively (35 pages). Ordering information is given on any current masthead page.

Notes

Contribution from the Department of Chemistry, University of Otago, P.O. Box 56, Dunedin, New Zealand

Stereochemical Change in the Hg^{2+}-, Ag^+-, and Cl_2-Induced and Spontaneous Reactions of Pentaamminecobalt(III)-Acido Species: A Reexamination

Nicola E. Brasch, David A. Buckingham,* Charles R. Clark, and Kim S. Finnie

Received February 16, 1989

Some 20 years ago we demonstrated by ^1H NMR spectroscopy the essential retention of stereochemistry when *trans*-$[Co(NH_3)_4(ND_3)X]^{2+}$ species ($X = N_3^-$, $NH_2CO_2^-$, Cl^-, Br^-) were treated with NO^+ or Hg^{2+} in the replacement of coordinated X^- by H_2O,[1] viz.

$$trans\text{-}[Co(NH_3)_4(ND_3)X]^{2+} + NO^+ \rightarrow trans\text{-}[Co(NH_3)_4(ND_3)OH_2]^{3+} + N_2 + N_2O \quad (1)$$

$$X = N_3^-, OCONH_2^-$$

$$trans\text{-}[Co(NH_3)_4(ND_3)X]^{2+} + Hg^{2+} \rightarrow trans\text{-}[Co(NH_3)_4(ND_3)OH_2]^{3+} + HgX^+ \quad (2)$$

$$X = Cl^-, Br^-$$

A similar result was found for the slower spontaneous aquation reaction (at 45 °C)

$$trans\text{-}[Co(NH_3)_4(ND_3)Br]^{2+} + H_2O \rightarrow trans\text{-}[Co(NH_3)_4(ND_3)OH_2]^{3+} + Br^- \quad (3)$$

Although not high by today's standards (a 60-MHz instrument was used), the quality of the data sufficed to distinguish the absence of major stereochemical change, and the results were interpreted in terms of dissociative S_N1 chemistry with formation of square-pyramidal intermediates as opposed to those of the trigonal-bipyramidal variety.

Since then extensive evidence has accumulated substantiating the dissociative nature of these reactions, and the focus of attention has shifted to evaluating the lifetime of the five-coordinate intermediate or intermediates so formed.[2] This cannot be very long since they appear to capture their immediate solvent–anion surroundings, and in some cases the reactions retain a small leaving-group dependence because of this. It also appears[3] that the major part of anion incorporation (i.e. in competition experiments when another group Y^- is available for entry) arises by direct association of Y^- with the inducing agent (i.e. as NOY, HgY^+, or ClCl in Cl_2 oxidation experiments).

(1) Buckingham, D. A.; Olsen, I. I.; Sargeson, A. M. *Aust. J. Chem.* **1967**, *20*, 597.

(2) Jackson, W. G.; McGregor, B. C.; Jurisson, S. S. *Inorg. Chem.* **1987**, *26*, 1286. This recent article lists most previous references on this topic and gives an account of the problems of mechanism that remain.

(3) Buckingham, D. A.; Clark, C. R.; Webley, W. S. *Inorg. Chem.* **1982**, *21*, 3353. This article discusses in some detail the anion dependence of the NO^+-induced reaction, but we were not the first to observe this (Haim, A.; Taube, H. *Inorg. Chem.* **1963**, *2*, 1199). Early publications also describe kinetic contributions from anions in the Hg^{2+} (Posey, F. A.; Taube, H. *J. Am. Chem. Soc.* **1957**, *79*, 255) and Ag^+ (Dolbear, G. E.; Taube, H. *Inorg. Chem.* **1967**, *6*, 60) cata Our own recent work in this area (unpublished) shows that anion contributions dominate the rate laws and products for the Hg^{2+}- and Ag^+-induced reactions, with anion-independent processes being of very minor importance.

0020-1669/89/1328-3386$01.50/0